

Dynamic Virtual Machine Management via Approximate Markov Decision Process

Zhenhua Han^{*†§}, Haisheng Tan[†], Guihai Chen[†], Rui Wang^{*}, Yifan Chen^{*}, Francis C.M. Lau[§]

^{*} South U. of Sci. & Tech. of China

[†] Jinan University, Guangzhou

[‡] Shanghai Jiao Tong University

[§] The University of Hong Kong

Abstract—Efficient virtual machine (VM) management can dramatically reduce energy consumption in data centers. Existing VM management algorithms fall into two categories based on whether the VMs’ resource demands are assumed to be static or dynamic. The former category fails to maximize the resource utilization as they cannot adapt to the dynamic nature of VMs’ resource demands. Most approaches in the latter category are heuristical and lack theoretical performance guarantees. In this work, we formulate dynamic VM management as a large-scale Markov Decision Process (MDP) problem and derive an optimal solution. Our analysis of real-world data traces supports our choice of the modeling approach. However, solving the large-scale MDP problem suffers from the curse of dimensionality. Therefore, we further exploit the special structure of the problem and propose an approximate MDP-based dynamic VM management method, called MadVM. We prove the convergence of MadVM and analyze the bound of its approximation error. Moreover, MadVM can be implemented in a distributed system, which should suit the needs of real data centers. Extensive simulations based on two real-world workload traces show that MadVM achieves significant performance gains over two existing baseline approaches in power consumption, resource shortage and the number of VM migrations. Specifically, the more intensely the resource demands fluctuate, the more MadVM outperforms.

I. INTRODUCTION

Virtual machine (VM) is a widely-used technology for data center management. By adopting virtualization-based solutions, servers could generate VMs according to users’ requests for storage space, computing resources (CPU cores or CPU time) and network bandwidth. Since multiple VMs could co-exist in a single server, virtualization could improve the utilization of the underloaded servers, which leads to reduced power consumption as fewer servers are used. Energy-efficient resource management for virtualization-based data centers has thus become an attractive research area.

In the literature, energy-efficient VM management in data centers can be divided into two categories based on whether the resource demands of the VMs are static or dynamic over time. If resource demand is treated as constant, the management problem can be formulated as a bin-packing problem [1]–[7]. Since in reality resource demands of VMs are essentially dynamic, static approaches would have low resource

utilization. When the resource demands of VMs are dynamic, it may happen that insufficient resources are provided to the VMs (called service-level agreement (SLA) violation or resource shortage). Thus, the allocation and migration policies of VMs should be made adaptive to such situations by jointly considering energy consumption and resource shortage over time. Jin et al. [8] modeled the resource demands of VMs as a normal distribution and proposed a stochastic bin-packing algorithm. They assumed that the statistics of the stochastic demands could be known, which is hard in practice. Some other works (e.g., [9], [10]) predicted the resource demands of VMs with historical data, which aimed mainly to avoid resource shortage, but have not considered the possibility of saving energy with VM migrations. Beloglazov et al. [11] proposed an algorithm for VM consolidation that jointly considered energy consumption, QoS and migration costs. They pursued the optimization of energy consumption at a time point rather than over a long period. Chen et al. [12] predicted the resource demand pattern for the initial VM placement, and migrated the VMs when the prediction turned out to be wrong. It is obvious that the accuracy of the prediction will degrade over time, and so will the resource utilization.

When considering dynamic resource demand, existing approaches of VM management are all centralized [8]–[13]. The data center would be in a panic when the centralized controller breaks down. Moreover, most of the dynamic approaches are heuristics-based, hence lack sufficient theoretical performance guarantee. In this paper, we regard the VM management as a stochastic optimization problem. Our analysis of real-world data traces shows that by properly choosing the time-slot duration, the first-order transition probability of the VMs’ resource demands is quasi-static for a long period and non-uniformly distributed, and hence the Markov chain model would be a simple and effective tool to capture the temporal correlations of the demands. Therefore, we adopt the Markov chain model to study the VM management problem, for which we jointly consider energy consumption and resource shortage. Our contributions can be summarized as follows:

- We formulate the dynamic VM management problem as an infinite horizon large-scale Markov Decision Process (MDP) problem with an objective to minimize the long-term average cost, the weighted sum of the power consumption and resource shortage. By solving

This is the full version of the paper appeared in INFOCOM’16.

Part of Z. Han’s work was done when he was visiting at Jinan University. Contact Haisheng Tan at thstan@jnu.edu.cn.

This work is supported in part by NSFC Grants 61502201, 61401192, 61472252, China 973 project (2014CB340303), Hong Kong RGC CRF Grant C7036-15G, and NSF-Guangdong Grant 2014A030310172.

the equivalent Bellman's equation, we propose an optimal VM management method with a time complexity that is exponential of the number of VMs.

- We propose an approximate MDP-based dynamic VM management algorithm, called MadVM. Moreover, we prove the convergence of MadVM and analyze the bound on the gap from the optimal solution. Moreover, our approach can be implemented in a distributed system with very little global information, and can therefore improve the robustness and scalability of data centers.
- We conduct detailed simulations based on two real-world workload traces. The experimental results show that MadVM can achieve significant performance gains over other existing algorithms in power consumption, resource shortage and the number of VM migrations, i.e., while maintaining the near-0 resource shortage, MadVM can reduce the power consumption by up to 23% and 47% (averagely 19% and 42%) compared with CompVM [12] and CloudScale [10], respectively.

The remainder of this paper is organized as follows. In Section II, we define the system model and the dynamic VM management problem. In Section III, we derive optimal and approximate algorithms for the problem. In Section IV, we analyze the temporal correlation of resource demands in Google data centers to validate our choice of using the Markov chain model. We evaluate the performance of our approach using the real-world data traces by comparing with other existing approaches. We conclude the paper in Section V.

II. SYSTEM MODEL AND PROBLEM DEFINITIONS

In this section, we define the system model, the power consumption model as well as the VM migration model, and formulate our dynamic VM management problem.

A. System Architecture

We consider a large-scale data center with a collection of physical servers (also called Physical Machines, PMs), where VMs are generated to run in a server according to the users' requests. Each VM is allocated to one PM, whereas a PM can be allocated multiple VMs. We assume there is a centralized manager to handle the allocation and migration of VMs.

For convenience, we assume that there are sufficient memory and network capacity for the VMs in each server. Only the scheduling of computational power (CPU time) is considered as it is the main factor determining the power consumption of the servers [14].¹ We assume the resource capacity of each server is identical, which is denoted as T_r . Different VM allocations will lead to different CPU utilizations and power consumptions. Thus, the centralized manager should be carefully designed to schedule allocation of VMs for power conservation. A slotted scheduling framework is adopted, where time is divided into a sequence of time-slots of the same

¹Note that through extending the dimensions of the state space \mathbb{Q} , our solution can be extended to multiple resources allocation, e.g., the CPU time, memory, and network bandwidth.

duration. At the beginning of a time-slot, each VM determines and submits its demand for CPU to the manager.

Let $V_m \triangleq \{m_1, \dots, m_{|V_m|}\}$ and $V_s \triangleq \{s_1, \dots, s_{|V_s|}\}$ denote the sets of VMs and PMs, respectively. Set $R_l(t)$ as the demand for CPU time of VM m_l at time t . Let $Y_i(t)$ denote the location of the VM m_i at time-slot t , i.e. $Y_i(t) = s_j$ if m_i is allocated to PM s_j . We set $\mathbf{Y}(t) \triangleq [Y_1(t), \dots, Y_{|V_m|}(t)] \in \mathbb{Y}$ as the aggregation of the locations of VMs, where \mathbb{Y} is the set of all possible $\mathbf{Y}(t)$. The aggregation of the demands from all VMs can be represented as a vector $\mathbf{R}(t) \triangleq [R_1(t), \dots, R_{|V_m|}(t)]$. We assume that resource demand is quantized into Λ discrete levels. Hence, we define $R_l(t) \in \mathcal{R}$, where $\mathcal{R} = \{r_0, r_1, \dots, r_{\Lambda-1}\}$.

We adopt the finite-state stationary Markov chain to model the resource demand and to capture its temporal correlation. The model $\mathbf{R}(t)$ is formulated with the following parameters,

- The state space of the resource demand is given by $\mathbf{R}(t) \in \mathbb{Q}$, where $\mathbb{Q} = \{\eta_1, \dots, \eta_{|\mathbb{Q}|}\}$. One item $\eta_i \in \mathbb{Q}$ is a vector of the demands from all VMs, denoted as $\eta_i = [\eta_{i,1}, \dots, \eta_{i,|V_m|}]$, where $\eta_{i,l}$ is the demand from VM m_l at state η_i .
- The transition kernel is given by

$$\begin{aligned} \phi_{i,j} &\triangleq \Pr[\mathbf{R}(t+1) = \eta_j | \mathbf{R}(t) = \eta_i] \\ &= \prod_{l=1}^{|V_m|} \Pr[R_l(t) = \eta_{i,l} | R_l(t-1) = \eta_{j,l}]. \end{aligned} \quad (1)$$

Here we assume the demands from different VMs are independent. By defining

$$\phi_{i,j,l} \triangleq \Pr[\eta_{i,l} | \eta_{j,l}], \quad (2)$$

we have $\phi_{i,j} = \prod_{l=1}^{|V_m|} \phi_{i,j,l}$.

Remark 1 (The motivation of the Markov chain model). *The resource demands of VMs may not follow a Markov chain strictly. However, they would have some of the common features of Markov chain. For example, the probability of the next CPU demand partly depends on the request of the current slot, and this transition probability is quasi-static within a coherent period. These features will be justified in Section IV-A by analyzing a real long-term workload data trace from Google, which is frequently used in the literature (e.g. [12], [15]). Therefore, the Markov chain model of a VM's demands can be treated as an approximation of the real world, capturing the temporal correlation of system dynamics.* ■

B. Power Consumption Model

The linear approximation model [14], widely adopted in the literature, is used to evaluate the power consumption of servers. The power consumption of server s_i is defined as

$$P_{s_i}(t) = P_{idle} + (P_{max} - P_{idle}) \cdot \min\left\{\frac{\sum_{\{l|Y_l(t)=s_i\}} R_l(t)}{T_r}, 1\right\},$$

where P_{idle} is the power consumption when the server is in the idle state (no computation task), and P_{max} is the consumption

in the fully-loaded state (100% utilization of CPU). If s_i is not allocated with any VM, it would be in sleep mode with a relatively low power consumption, $P_{sleep} \ll P_{idle}$. The total power consumption of the servers in the data center at time t is

$$P_{total}(t) = \sum_{s_i \in V_s} P_{s_i}(t). \quad (3)$$

Due to the dynamics of resource demands of VMs, the changes in power consumption form a stochastic process. If some VMs have low resource demand with high probability, the centralized manager can consolidate them into fewer PMs. In contrast, when some VMs work at high resource demand with high probability, VM migrations should be initiated to allocate more PMs to these VMs so that resource shortage can be avoided.

C. VM migration

VM migration, which is to move a running VM from one PM to another without disconnecting the clients or applications, is a basic operation supported by many platforms, such as Xen [16] and KVM [17]. In each time-slot, the data center manager determines which VMs should be migrated and the PMs they should migrate to. We denote $\gamma(t) \triangleq [\gamma_1(t), \dots, \gamma_{|V_m|}(t)] \in \mathcal{A}$ as the migration of the VMs at the t^{th} time-slot, where \mathcal{A} is the set of feasible migration actions and $\gamma_l(t)$ is the target PM of m_l after migration. We define \mathcal{A}_l as the set of available migration actions of m_l , i.e. $\gamma_l \in \mathcal{A}_l$. We assume the migration can be finished in one time-slot. Thus, the location of m_i will be γ_i in the next time-slot, i.e. $Y_i(t+1) = \gamma_i$. If m_i is not migrated at the t^{th} time-slot, we have $Y_i(t) = Y_i(t+1) = \gamma_i(t)$.

VM migrations will result in many data transmissions consuming a large amount of network bandwidth; so we set the maximum number of migrated VMs in one time-slot as T_m , i.e.,

$$\sum_{i=1}^{|V_m|} \mathbf{1}[\gamma_i(t) \neq Y_i(t)] \leq T_m, \quad (4)$$

where $\mathbf{1}[\cdot]$ is the indicator function which is equal to 1 when the condition holds, and 0 otherwise.

D. Problem Formulation

Our aim is to optimize the average power consumption and the resource shortage over a long period given the dynamic resource demands from VMs. Here, we formulate our VM management task as an MDP problem, where the system state is defined as follows.

Definition 1 (System State). *The system state at the t^{th} time-slot can be uniquely specified by*

$$\mathbf{S}(t) \triangleq [\mathbf{R}(t), \mathbf{Y}(t)] \in \mathbb{S}, \quad (5)$$

where $\mathbb{S} = \mathbb{Q} \times \mathbb{Y}$ denotes the space of the system states.

At the beginning of each time-slot (say the t^{th} time-slot), the data center manager would collect the system information $\mathbf{S}(t)$ and determine the control action for each VM.

Definition 2 (Stationary Control Policy). *A stationary control policy Ω is a mapping from the system state \mathbf{S} to the VM migration actions, i.e. $\Omega(\mathbf{S}(t)) = \gamma(t)$ at the t^{th} time-slot.*

To quantify the resource shortage (i.e., the amount of resource demand that is not satisfied), we define the shortage level θ_i for the i^{th} PM at time t as

$$\theta_i(t) \triangleq \max\left\{\frac{\sum_{\{l|Y_l(t)=s_i\}} R_l(t)}{T_r} - 1, 0\right\}, \quad (6)$$

Instead of achieving instantaneous optimality, we focus on seeking an optimal control policy to minimize the cost as a long-term average. The total power consumption as a long-term average can be defined as follows,

$$\overline{P_{total}}(\Omega) \triangleq \lim_{T \rightarrow +\infty} \mathbb{E}_{\Omega} \left[\frac{1}{T} \sum_{t=1}^T P_{total}(t) \right], \quad (7)$$

where $\mathbb{E}_{\Omega}[\cdot]$ is the expectation under the stationary control policy Ω . Similarly, we denote $\bar{\theta}$ as the average (per-VM) resource shortage level in long-term average, which is

$$\bar{\theta}(\Omega) \triangleq \lim_{T \rightarrow +\infty} \mathbb{E}_{\Omega} \left[\frac{1}{T \cdot |V_m|} \sum_{i=1}^{|V_s|} \sum_{t=1}^T \theta_i(t) \right]. \quad (8)$$

Considering power consumption and resource shortage simultaneously, we define the instantaneous cost by jointly combining the two objectives as follows:

$$g(t) \triangleq P_{total}(t) + \frac{\lambda}{|V_m|} \cdot \sum_{i=1}^{|V_s|} \theta_i(t), \quad (9)$$

where λ is the weight of resource shortage.²

Finally, we define our problem as follows:

Problem 1 (The Dynamic VM Management Problem).

$$\begin{aligned} \min_{\Omega} \quad & \bar{g}(\Omega) = \lim_{T \rightarrow +\infty} \mathbb{E}_{\Omega} \left[\frac{1}{T} g(t) \right] \\ & = \overline{P_{total}}(\Omega) + \lambda \cdot \bar{\theta}(\Omega) \quad (10) \\ \text{s.t.} \quad & (4) \quad \forall t \quad (11) \end{aligned}$$

where the goal $\bar{g}(\Omega)$ is defined as the long-term average cost of Eqn. (9) under the control policy Ω . The constraint is the maximum number of VM migrations allowed in one time-slot.

For a given λ , the solution to Problem 1 corresponds to a point in the Pareto optimal tradeoff curve between the average power consumption and the average resource shortage.

²The weight λ indicates the relative importance of the resource shortage over the power consumption. It can be interpreted as the corresponding Lagrange multiplier associated with the resource shortage constraint. If the system does not allow resource shortage, we can set $\lambda = +\infty$. We study the influence of the setting of λ in Section IV-C by simulations.

III. MDP-BASED DYNAMIC VM MANAGEMENT ALGORITHMS

In this section, we propose an optimal MDP-based algorithm to solve the dynamic VM management problem as just formulated. To avoid the curse of dimensionality, we derive another approximate algorithm based on the optimal solution using the local dynamic resource demand of each VM. We then prove the convergence of the proposed algorithm and derive the bound of the approximation error compared with the optimal.

A. Optimal VM Management Algorithm

Since we focus on minimizing the average cost over time, we formulate the dynamic VM management in Problem 1 as an infinite horizon average MDP. The optimal solution can be achieved by solving the equivalent Bellman's equation [18].

Lemma 1 (Equivalent Bellman's Equation). *If a scalar β and a vector of the utility function $\mathbf{V} = [V(S_1), V(S_2), \dots]$ satisfy the Bellman's equation for Problem 1, written as $\forall S_i \in \mathbb{S}$,*

$$\beta + V(S_i) = \min_{\gamma \in \mathcal{A}(S_i)} \left[g(S_i) + \sum_{S_j \in \mathbb{S}} Pr[S_j|S_i, \gamma] V(S_j) \right], \quad (12)$$

where $g(S_i)$ is the instantaneous cost under the system state S_i , then β is the optimal average cost:

$$\beta = \min_{\Omega} \bar{g}(\Omega). \quad (13)$$

Moreover, Ω is the optimal control policy if it attains the minimum in the R.H.S. of Eqn. (12). ■

Given the control policy Ω , the transition probability of the system state $\mathbf{S}(t)$ at the t^{th} time-slot can be written as

$$\begin{aligned} & Pr[\mathbf{S}(t+1) | \mathbf{S}(t), \Omega(\mathbf{S}(t))] \\ &= Pr[\mathbf{R}(t+1), \mathbf{Y}(t+1) | \mathbf{R}(t), \mathbf{Y}(t), \Omega(\mathbf{S}(t))] \\ &= Pr[\mathbf{R}(t+1) | \mathbf{R}(t)] Pr[\mathbf{Y}(t+1) | \mathbf{Y}(t), \Omega(\mathbf{S}(t))] \\ &= Pr[\mathbf{R}(t+1) = \eta_i | \mathbf{R}(t) = \eta_j] \\ &= \phi_{i,j} \quad (\text{the transition kernel defined in Eqn.(1)}), \end{aligned} \quad (14)$$

where the third line means the migration action of VMs is deterministic, i.e., $Pr[\mathbf{Y}(t+1) | \mathbf{Y}(t), \Omega(\mathbf{S}(t))] = 1$. Note that the transition kernel is unknown to the data center manager. However, it can be learned by combining the sliding window scheme and the maximum likelihood estimation (MLE) [13]. Recall that we assume the transition of resource demand is independent among the VMs. We can capture the temporal correlation of a VM's resource demands by estimating $\phi_{i,j,l}$ as defined in Eqn. (2). Denote the estimated $\phi_{i,j}$ and $\phi_{i,j,l}$ as $\hat{\phi}_{i,j}$ and $\hat{\phi}_{i,j,l}$, respectively. We can learn $\hat{\phi}_{i,j,l}$ as follows:

$$\hat{\phi}_{i,j,l}(t) = \frac{\sum_{t'=t-T_w+1}^t \mathbf{1}[R_l(t'-1) = r_i]}{\sum_{t'=t-T_w+1}^t \mathbf{1}[R_l(t'-1) = r_i | R_l(t') = r_j]}, \quad (15)$$

Algorithm 1: Compute the Optimal Utility Function in Lemma 1 by Value Iteration

Input: The estimated transition probabilities $\hat{\phi}_{i,j}(t)$, $\forall i, j$
Output: The optimal utility function $V(\cdot)$

- 1 $\hat{t} = 0$, $V^0(S_i) = 0, \forall S_i \in \mathbb{S}$;
- 2 **while** Not converge **do**
- 3 $\hat{t} = \hat{t} + 1$;
- 4 **for** $S_i \in \mathbb{S}$ **do**
- 5 $V^{\hat{t}}(S_i) = \min_{\gamma \in \mathcal{A}(S_i)} \left\{ g(S_i) + \sum_{S_j \in \mathbb{S}} Pr[S_j|S_i, \gamma] \cdot V^{\hat{t}-1}(S_j) \right\}$;
- 6 **for** $S_i \in \mathbb{S}$ and $S_i \neq S_r$ **do**
- 7 $V^{\hat{t}}(S_i) = V^{\hat{t}}(S_i) - V^{\hat{t}}(S_r)$;
- 8 $S_r = 0$;

where T_w is the length of the sliding window and $r_{i,l}$ is the demand level of m_l in state η_i .

Bellman's equation in Lemma 1 is a fixed-point problem in a functional space. Given the estimated transition probability $\hat{\phi}_{i,j}$, the Bellman's equation can be solved with value iteration or policy iteration [19], which is a general solution to calculate the optimal utility function iteratively. We demonstrate the procedure of value iteration to compute the optimal utility function \mathbf{V} in Algorithm 1. In each iteration, the utility function will be updated to $V^{\hat{t}}$ by finding the optimal policy under the previous function $V^{\hat{t}-1}$ (Lines 4 to 5). The function \mathbf{V} will converge to the optimal utility function which satisfies Lemma 1. Before the convergence, it has been proved that the utility function keeps increasing in each iteration. Thus, the utility function may converge to a large value. We choose a reference state S_r which can be any fixed state in the space \mathbb{S} . In each iteration, the utility function for a state is replaced by the relative value to that of the reference state (Line 6 to Line 8). This operation can avoid the utility function converging to a very large value, while not changing the optimal control policy found after convergence. Due to the limited space, readers can refer to [18] for a better understanding of value iteration. After obtaining the utility function, we can find the optimal control policy by the R.H.S. of Eqn. (12) in Lemma 1.

It is NP-hard to solve the Bellman's equation [20]. Algorithm 1 traverses all the states in \mathbb{S} , and needs exponential time and space to compute the utility function. We propose an efficient approximate algorithm in the following subsections.

B. Per-VM Utility Function

To avoid the curse of dimensionality, we have to reduce the state space of the utility function. Instead of making all the states satisfy the Bellman's equation in Eqn. (12), we choose to satisfy a few of the states, called the *key states*. Before describing how to find the key states, we define the *feature state*, denoted as $f_l(t)$, for VM m_l at time t . The feature state $f_l(t)$ is the combination of the location of m_l and its expected

resource demand in the steady distribution of R_l which is denoted as

$$\pi_l^\infty = \lim_{n \rightarrow \infty} \pi_l^0 (\mathbf{P}_l)^n, \quad (16)$$

where π_l^0 is a row vector ($\pi_l^0(i) = 1$ iff $R_l = r_i$, and $\pi_l^0(i) = 0$ otherwise), and \mathbf{P}_l is the transition probability matrix of resource demand of m_l . Then, we have

$$f_l(t) = \left(\left[\sum_{i=0}^{\Lambda-1} r_i \cdot \pi_l^\infty(i) \right], Y_l(t) \right). \quad (17)$$

Based on the above, the key states for the VM m_l at time-slot t , denoted as \mathbf{S}_K^l , are defined as following,

$$\mathbf{S}_K^l = \{i_{l,r,y}(t) | r = r_0, \dots, r_{\Lambda-1}; y = s_1, \dots, s_{|V_s|}\}, \quad (18)$$

where $i_{l,r,y}(t) = [S_1 = f_1(t), S_2 = f_2(t), \dots, S_l = [r, y], \dots, S_{|V_m|} = f_{|V_m|}(t)]$ denotes the state with $S_l = [r, y]$ and $S_i = f_i(t)$ ($\forall i \neq l$). We denote \mathbf{S}_K as the set of the key states satisfying the Bellman's equation in Eqn. (12), which is written as $\mathbf{S}_K = \bigcup_{l=1}^{|V_m|} \mathbf{S}_K^l$.

At each time-slot t , for the VM m_l , we define the per-VM utility function $\tilde{V}_l(i_{l,r,y}(t))$ as the utility function of the key state $i_{l,r,y}(t)$, which satisfies, $\forall S_i \in \mathbf{S}_K^l$

$$\beta_l + \tilde{V}_l(S_i) = \min_{\gamma_l \in \mathcal{A}_l(S_i)} \left\{ g(S_i) + \sum_{S_j \in \mathbf{S}_K^l} Pr[S_j | S_i, \gamma_l] \tilde{V}_l(S_j) \right\}. \quad (19)$$

Here, β_l is the optimal cost derived from the local key states \mathbf{S}_K^l and the local control action \mathcal{A}_l . For ease of notation, we denote $\tilde{V}_l(i_{l,r,y})$ as $\tilde{V}_l(r, y)$. We denote $\tilde{\mathbf{V}}_l \triangleq [\tilde{V}_l(r_0, s_1), \dots, \tilde{V}_l(r_{\Lambda-1}, s_{|V_s|})]^T$ ($l = 1, \dots, |V_m|$) as the per-VM utility function vector for all key states of each VM.

We adopt a feature-based method to approximate the utility function $V(\mathbf{S})$ as a linear summation of the per-VM utility functions, and each VM updates its per-VM utility function with local state information as well as the feature state of other VMs. Specifically, the proposed linear approximation of the utility function $V(\mathbf{S})$ is given by

$$\begin{aligned} V(\mathbf{S}) &= V([S_1, \dots, S_{|V_m|}]) \\ &\approx \sum_{l=1}^{|V_m|} \sum_{i=0}^{\Lambda-1} \sum_{j=1}^{|V_s|} \tilde{V}_l([r_i, s_j]) \mathbf{1}[R_l = r_i, Y_l = s_j] \\ &= \mathbf{W}^T \mathbf{F}(\mathbf{S}), \end{aligned} \quad (20)$$

where the parameter vector \mathbf{W} and the feature vector \mathbf{F} are given by Eqn. (21) and Eqn. (22), respectively.

$$\mathbf{W} \triangleq [\tilde{V}_0(r_0, s_1), \dots, \tilde{V}_0(r_{\Lambda-1}, s_{|V_s|}), \tilde{V}_1(r_0, s_1), \dots, \tilde{V}_{|V_m|}(r_{\Lambda-1}, s_{|V_s|})]^T, \quad (21)$$

$$\mathbf{F}(\mathbf{S}) \triangleq [\mathbf{1}[R_0 = r_0, Y_0 = s_1], \dots, \mathbf{1}[R_0 = r_{\Lambda-1}, Y_0 = s_{|V_s|}], \mathbf{1}[R_1 = r_0, Y_1 = s_1], \dots, \mathbf{1}[R_{|V_m|} = r_{\Lambda-1}, Y_{|V_m|} = s_{|V_s|}]]^T. \quad (22)$$

For example, suppose there are three VMs and two PMs. We set the number of resource demand levels as $\Lambda = 2$. At time-slot t , the system state $\mathbf{S}(t)$ is $[S_1(t) = [r_0, s_1], S_2(t) = [r_1, s_1], S_3(t) = [r_0, s_2]]$. Thus the utility function $V(\mathbf{S}(t))$ can be given by the linear approximation, as follows:

$$\begin{aligned} V(\mathbf{S}(t)) &\approx \tilde{V}_1(S_1(t)) + \tilde{V}_2(S_2(t)) + \tilde{V}_3(S_3(t)) \\ &= \tilde{V}_1(r_0, s_1) + \tilde{V}_2(r_1, s_1) + \tilde{V}_3(r_0, s_2). \end{aligned}$$

We can find that the state space is dramatically reduced from exponential to polynomial with the linear approximation. However, the space of control actions is still exponential due to the joint actions of all VMs. In the following lemma, we exploit the equivalent Bellman's equation in Eqn. (12) to show that the space of control actions can also be reduced to polynomial by decomposing the joint control actions into the individual control action of each VM.

Lemma 2. *After the linear approximation in Eqn. (20), the equivalent Bellman's equation in Eqn. (12) can be approximately computed as $\forall S_i \in \mathbf{S}$*

$$\begin{aligned} \beta + V(S_i) &= \min_{\gamma \in \mathcal{A}(\mathbf{S}_i)} \left\{ g(S_i) + \sum_{S_j \in \mathbf{S}} Pr[S_j | S_i, \gamma] V(S_j) \right\} \\ &\approx \sum_{l=1}^{|V_m|} \left(g(S_i) + \min_{\gamma_l \in \mathcal{A}_l(\mathbf{S}_i)} \left\{ \sum_{S'_j \in \mathbf{S}_K^l} Pr[S'_j | S_i, \gamma_l] \tilde{V}_l(S'_j) \right\} \right) \end{aligned}$$

Proof. Refer to Appendix A. \square

C. Approximate Algorithm: MadVM

Based on the above, we now describe our approximate Markov-Decision-Process-based dynamic VM management algorithm for Problem 1, called MadVM. We first assume there is a centralized manager that determines the control policy, and then demonstrate how to implement our algorithm in a distributed system. MadVM consists of five main steps that are executed sequentially, each in a time-slot:

- **Step 1, Initialization:** At the beginning of a time-slot t , the centralized manager initializes the per-VM utility function for each VM, i.e. $\tilde{V}_l(S_i) = 0$ ($l = 1, \dots, |V_m|, \forall S_i \in \mathbf{S}_K^l$).
- **Step 2, Updating the Transition Probabilities:** Each VM updates the transition probabilities of the resource demand according to Eqn. (15), and then determines its feature state f_l according to Eqn. (17).
- **Step 3, Information Collection of the Centralized Manager:** For each VM m_l , the manager collects its resource demand $R_l(t)$, the matrix of transition probability \mathbf{P}_l and the feature state $f_l(t)$.
- **Step 4, Calculating the Per-VM Utility Function:** Based on the feature states, the centralized manager calculates the per-VM utility function \tilde{V}_l for each VM m_l . The computation is similar to the optimal value iteration in Algorithm 1 while the state space and utility function are replaced by the per-VM key states and per-VM utility

function respectively, i.e. the operation from Line 4 to Line 5 is replaced by $\forall l = 1, \dots, |V_m|, \forall S_i \in \mathbf{S}_K^l$

$$\tilde{V}^l(S_i) = \min_{\gamma_l \in \mathcal{A}_l(S_i)} \left\{ g(S_i) + \sum_{S_j \in \mathbf{S}_K^l} Pr[S_j|S_i, \gamma_l] \cdot \tilde{V}^{l-1}(S_j) \right\} \quad (23)$$

And, the reference state S_r in Line 8 is replaced by state formed by the feature states of all VMs, i.e.

$$S_r = [S_1 = f_1(t), S_2 = f_2(t), \dots, S_{|V_m|} = f_{|V_m|}(t)]$$

- **Step 5, Determining the Control Actions:** We define the control utility V_l^c for VM m_l as the control action under the current system state $\mathbf{S}(t)$, which is

$$V_l^c(\mathbf{S}(t)) = \min_{\gamma_l \in \mathcal{A}_l(\mathbf{S}(t))} \left\{ g(\mathbf{S}(t)) + \sum_{S_j \in \mathbf{S}_K^l} Pr[S_j|\mathbf{S}(t), \gamma_l] \cdot \tilde{V}_l(S_j) \right\}, \quad (24)$$

The corresponding control action is the migration action which attains the minimum in the R.H.S. of Eqn. (24). The centralized manager would rank the control utilities in ascending order, and choose the top T_m migration as the control action in time t . Then, it goes back to Step 1 for time $t + 1$. ■

We can see MadVM has the following two distinct merits:

1) *Low Complexity:* In MadVM, only the local states and feature states are used to update the per-VM utility function, and hence the state space is $\Theta(|V_m||V_s| \cdot \Lambda)$. Moreover, the space of control actions in Eqn. (24) is also simplified from $\Theta(|V_s||V_m|)$ to $\Theta(|V_s|)$. Therefore, the complexity is reduced significantly from exponential to polynomial.

2) *Implementation in a distributed system:* MadVM can be implemented in a distributed system with a small amount of information sharing. At the 3rd step of any time t , one VM m_l shares essential information to the other VMs, including its feature state f_l and the current state $S_l(t)$. Note that the matrix of transition probability \mathbf{P}_l need not be shared since the other VMs do not make use of it to update their utility functions. At the 4th step, each VM locally calculates the per-VM utility function of itself. At the 5th step, each VM, such as m_l , submits the control utilities $V_l^c(\mathbf{S}(t))$ to hold an auction. The top T_m VMs with the maximum control utility win the auction and proceed with their control actions.

D. Convergence Analysis

Since MadVM only makes partial system states satisfy Bellman's equation in Eqn. (12), the convergence of the approximate value iteration is still unknown. In this section, we prove that the approximate value iteration for updating per-VM utility function will indeed converge.

For each VM m_l , let $\tilde{\mathbf{P}}_\gamma^l$ denote the transition probability matrix under the control action γ , i.e. the (i, j) -th element of $\tilde{\mathbf{P}}_\gamma^l$ is $Pr[S_i|S_j, \gamma]$ ($\forall S_i, S_j \in \mathbf{S}_K^l$). We write $\tilde{\mathbf{P}}_\gamma^l$ as $\tilde{\mathbf{P}}_\gamma$ without ambiguity. We define the iteration operation (Line 5

in Algorithm 1) as the mapping functions \mathcal{F} , and \mathcal{F}_γ is given as

$$\mathcal{F}(\tilde{\mathbf{V}}_l) \triangleq \min_{\gamma} \{ \mathbf{g} + \tilde{\mathbf{P}}_\gamma \tilde{\mathbf{V}}_l \}, \text{ and} \quad (25)$$

$$\mathcal{F}_\gamma(\tilde{\mathbf{V}}_l) \triangleq \mathbf{g} + \tilde{\mathbf{P}}_\gamma \tilde{\mathbf{V}}_l, \quad (26)$$

where $\mathbf{g} = [g(i_l, r_0, s_1), \dots, g(i_l, r_{\Lambda-1}, s_{|V_s|})]$ is the vector of the cost of the local system states for VM m_l . We denote the value of the system state S_i in $\mathcal{F}_{\gamma_k}(\mathbf{V})$ as $\mathcal{F}_{(k)}(S_i)$, where γ_k is the control action determined in the k^{th} iteration. Therefore, the value iteration can be given by

$$\tilde{\mathbf{V}}_l^{k+1}(S_i) = \mathcal{F}_{(k)}(S_i) - \mathcal{F}_{(k)}(S_r), \quad \forall S_i \in \mathbf{S}_K^l. \quad (27)$$

We prove the convergence of the iterations to compute the per-VM utility function with the following theorem.

Theorem 1 (Convergence of the Per-VM Utility Function). *Let $\tilde{\mathbf{V}}_l^*$ be the optimal average cost vector in the per-VM utility function of VM m_l . The sequence of utility function $\{\tilde{\mathbf{V}}_l^k, k = 1, 2, \dots\}$ in iterations converges to $\tilde{\mathbf{V}}_l^*$ which satisfies*

$$\mathcal{F}(\tilde{\mathbf{V}}_l^*(S_r))\mathbf{e} + \tilde{\mathbf{V}}_l^* = \mathcal{F}(\tilde{\mathbf{V}}_l^*), \quad (28)$$

where $\mathbf{e} = (1, \dots, 1)^T$ is the unit vector.

Proof. Refer to Appendix B. It is similar to the proof of the optimality of value iteration for the undiscounted average cost problem in [18]. □

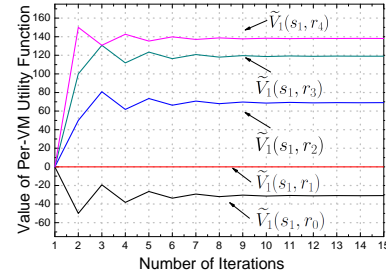


Fig. 1. Illustration of convergence: Per-VM utility function versus the number of iterations. There is one PM and one VM, i.e. $|V_s| = 1, |V_m| = 1$. The resource demand is quantized into 5 levels, i.e. $\Lambda = 5$.

Fig. 1 illustrates the convergence of the per-VM utility function by an example. We can see that the utility function converges before the 15th iteration, and its value increases while the resource demand grows.

E. Asymptotic Performance Analysis

We denote \mathbf{V}^* as the vector of the optimal utility function for each system state in the original system, which satisfies the equivalent Bellman's equation in Lemma 1. Although Theorem 1 asserts the convergence of the per-VM utility function, there is still an approximation error between the parameter vector \mathbf{W} and \mathbf{V}^* . Let $\mathbf{M} \in \mathbb{R}^{N_S \times (|V_s| \cdot \Lambda)}$ denote the mapping matrix from \mathbf{W} to the original system, where $N_S = (|V_s| \cdot \Lambda)^{|V_m|}$ is the number of the original system states. We set \mathbf{V}^\ddagger as the approximate utility function in the original system mapped from the parameter vector \mathbf{W} . Here, for a matrix \mathbf{H} , we denote its inverse as \mathbf{H}^\dagger . Therefore, we have

$$\mathbf{V}^\ddagger = \mathbf{M}\mathbf{W} \quad \text{and} \quad \mathbf{W} = \mathbf{M}^\dagger \mathbf{V}^\ddagger, \quad (29)$$

where $\mathbf{M}^\dagger \in \mathbb{R}^{|V_s| \Lambda \times N_s}$ has only one 1 in each row and the positions of 1s correspond to the positions of the key states.

In the following theorem, we provide a bound on the approximation error $\|\mathbf{M}\mathbf{W} - \mathbf{V}^*\|$, where $\|\cdot\|$ is the l^2 -norm of the vector.

Theorem 2 (Bound on the Approximation Error). *Let \mathbf{X}^* denote the optimal utility function after approximation which is $\mathbf{X}^* = \arg \min_{\mathbf{X}} \|\mathbf{M}\mathbf{X} - \mathbf{V}^*\| = (\mathbf{M}^T \mathbf{M})^\dagger \mathbf{M}^T \mathbf{V}^*$. The approximation error is lower-bounded by*

$$\|\mathbf{M}\mathbf{W} - \mathbf{V}^*\| \geq \|\mathbf{M}\mathbf{X}^* - \mathbf{V}^*\|, \quad (30)$$

and upper-bounded by

$$\|\mathbf{M}\mathbf{W} - \mathbf{V}^*\| \leq \frac{a(c^n + 1)}{1 - \beta} \|\mathbf{X}^* - \mathbf{M}^\dagger \mathbf{V}^*\| + \|\mathbf{M}\mathbf{X}^* - \mathbf{V}^*\|, \quad (31)$$

where $a = \sqrt{|V_m| \times (|V_s| \Lambda)^{|V_m|}}$, n is integer and $0 < \beta < 1$. n and β should satisfy

$$\|\mathcal{F}^n(\mathbf{W}) - \mathcal{F}^n(\mathbf{X}^*)\| \leq \beta \|\mathbf{W} - \mathbf{X}^*\|, \quad (32)$$

and c should satisfy

$$\begin{aligned} \|\mathcal{F}^m(\mathbf{W}) - \mathbf{M}^\dagger \mathbf{V}^*\| \\ \leq c \|\mathcal{F}^{m-1}(\mathbf{W}) - \mathbf{M}^\dagger \mathbf{V}^*\|, m = 1, 2, \dots, n. \end{aligned} \quad (33)$$

Proof. Refer to Appendix C. \square

Due to the convergence of the per-VM utility function in Theorem 1, we have $\lim_{k \rightarrow \infty} \mathcal{F}^k(\mathbf{X}^*) = \mathbf{W}$. Thus, there always exists a pair of (n, β) which satisfies $\|\mathcal{F}^n(\mathbf{W}) - \mathcal{F}^n(\mathbf{X}^*)\| \leq \beta \|\mathbf{W} - \mathbf{X}^*\|$. Intuitively, the pair of (n, β) measures the convergence speed of the value iteration such that smaller n or smaller β results in higher convergence speed.

Note that $\|\mathcal{F}^m(\mathbf{W}) - \mathbf{M}^\dagger \mathbf{V}^*\| = \|\mathbf{M}^\dagger \mathcal{F}^\dagger(\mathbf{M} \mathcal{F}^{m-1}(\mathbf{X}^*)) - \mathbf{M}^\dagger \mathcal{F}^\dagger(\mathbf{V}^*)\|$, where \mathcal{F}^\dagger is a contraction mapping on the key states \mathbf{S}_K . There always exists a sufficiently large $c \in [0, 1)$ such that $\|\mathcal{F}^m(\mathbf{W}) - \mathbf{M}^\dagger \mathbf{V}^*\| \leq c \|\mathcal{F}^{m-1}(\mathbf{W}) - \mathbf{M}^\dagger \mathbf{V}^*\|$. The constant c measures the contraction ratio of the contraction mapping \mathcal{F}^\dagger , such that the smaller c results in the larger contraction ratio.

In summary, if the value iteration operation \mathcal{F} has good convergence speed and the contraction mapping \mathcal{F}^\dagger has large contraction ratio on the key states \mathbf{S}_K , we will have a small upper-bound on approximation error. However, the approximation error can never be smaller than $\|\mathbf{M}\mathbf{X}^* - \mathbf{V}^*\|$ owing to the fundamental limitation on the vector dimension.

IV. PERFORMANCE EVALUATION

In this section, we first analyze the temporal correlations of the resource demands from VMs in Google's data centers. Then, we compare the performance of our dynamic VM management algorithm MadVM with two baseline algorithms using the data traces from Google Cluster [21] and PlanetLab [22]. The former data trace has a long duration of 26 days, and the latter has more intensely fluctuating resource demands from VMs.

A. Resource Demand from VMs in Google Data Centers

In MadVM, we adopt the Markov chain model to capture the temporal correlation of VM resource demands approximately. Here, we look into a real data trace [21] coming from Google data centers to validate the rationality of our model.

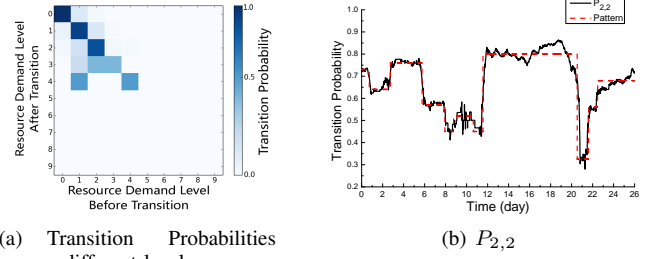


Fig. 2. Transition probability of CPU demand in Google data trace. We arbitrarily choose one among 3000 VMs for observation. The experiment results of other VMs are similar. Fig. 2(a) shows the transition probability matrix of CPU demand from the VM at a randomly selected time-slot. We divide the CPU resource demand into 10 levels. The transition probability is calculated by the maximum likelihood estimation shown in the Eqn. (15) with window size of 3 days. We can find that the resource demand is always less than half of a PM's capacity. Therefore, VM consolidation can evidently improve the utilization of PMs. Moreover, the transition probabilities of the demand level after transition are not uniformly distributed. Therefore, the demand at time-slot $(t+1)$ is closely dependent on that at time-slot t . The existence of temporal correlation proves the rationality of using the Markov chain model to characterize the resource demand.

Fig. 2(b) shows the variation of $P_{2,2}$, the probability that the demand level stays on r_2 at two consecutive time-slots, which is the 3rd row and the 3rd column in Fig. 2(a). Due to the limited space, we only take $P_{2,2}$ as an example here. Since the transition probabilities are strongly correlated to the behavior of the VM, the other transition probabilities also have the same characteristics as $P_{2,2}$. We can find that the transition probability always lingers around a value for several days (drawn as the red dash line in Fig. 2(b)). This phenomenon shows that the transition probability is quasi-static for a short-term, e.g. 3 days. Note that the value iteration in our algorithm MadVM will be executed every time-slot. Therefore, the control policy capturing the temporal correlation can always be obtained by our method according to the transition probabilities.

B. Performance Evaluation of MadVM

We have conducted simulations to evaluate the performance of MadVM using the VM utilization traces from Google Cluster and PlanetLab. We compare MadVM to two baseline methods for dynamic VM management, a well-known algorithm CloudScale [10] and a latest algorithm CompVM [12]. Both CompVM and CloudScale predict future resource demand to decide the control policy. In the initial VM allocation, MadVM and CloudScale place each VM to the first-fit PM based on the

expected VM resource demand, while CompVM first predicts the pattern of resource demand and then decide how to deploy the VMs to fully utilize the PMs.

In the experiments, one time-slot is set to 10 minutes. We configure the PMs in the system with the capacity of a quad-core 1.5GHz CPU, and VMs with the capacity of a single-core 1.5GHz. We set the powers for the fully-loaded state P_{max} , the idle state P_{idle} and the sleep state P_{sleep} to 500 watts, 250 watts and 50 watts, respectively. The window size is set to 3 days to calculate the transition probabilities in MadVM. The maximum number of VM migrations in one time-slot is set to 2% of the total number of VMs. We take the data of the first 6 days from the two traces in the following experiments. The numbers of VMs and physical machines are set as 1000 and 500 respectively. To evaluate the performance of the three methods, we use the following metrics measured in 6 days and take the average over the time-slots spanned (864 time-slots in total) : 1) *the average power consumption*: to evaluate the energy efficiency; 2) *the number of PMs used*: to illustrate the utilization of PMs; 3) *the average resource shortage*: to illustrate how much resource demand is not satisfied; and 4) *the average number of VM migrations*: to present the frequency of migrations.

In the following, we first demonstrate the impact of the parameter λ , and then compare MadVM with CompVM and CloudScale according to the above four metrics.

C. Performance with different λ

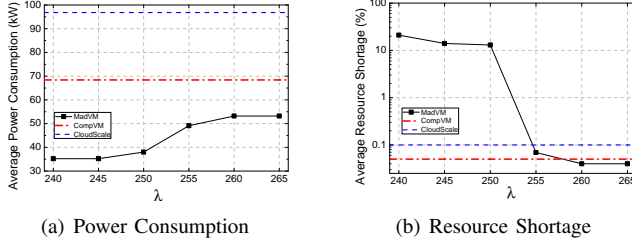


Fig. 3. Power consumption and resource shortage with different λ

In order to handle the tradeoff between power consumption and resource shortage, we introduce a parameter λ in our objective defined in Eqn. (9). Here, we investigate the relationship among λ , the average power consumption and the average resource shortage with the Google cluster trace. Fig.3 indicates when λ increases, the power consumption increases and the resource shortage decreases, which is reasonable since the larger λ , the greater the influence from the shortage. We also include the power consumption of CompVM and CloudScale under this data trace in Fig.3(a). We can see that MadVM has the best power efficiency, even when λ is set to a large number. Fig.3(b) demonstrates the resource shortage when λ changes (note that the vertical axis is in the logarithmic scale). We can see that the resource shortage of MadVM decreases dramatically when λ increases. As the resource demands from VMs are dynamic, resource shortage cannot be completely avoided. As shown in Fig.3(b), CompVM and CloudScale also

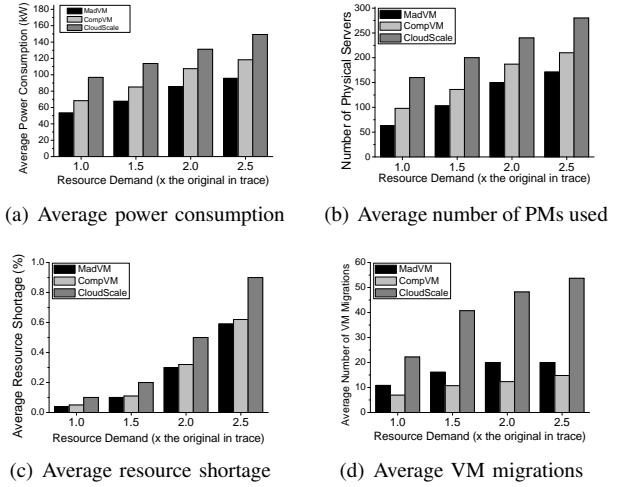


Fig. 4. Performance in the Google Cluster Trace

have a shortage rate that is nearly 0. When λ is large enough, i.e., $\lambda > 260$, our shortage is the smallest.

In the following simulations, we set λ to a very large value (i.e., $\lambda = 10^6$) so that our resource shortage is below the other two baseline algorithms.

D. Performance with different VM Resource Demand

Fig. 4 and 5 demonstrate the performance of three methods under different VM resource demands with the Google trace and the PlanetLab trace. The resource demand of the VMs is set to 1, 1.5, 2 and 2.5 times of the original in the traces.

Fig. 4(a) and Fig. 4(b) demonstrate the average power consumption and the average number of PMs used per time-slot in the Google cluster trace respectively. In Fig. 4(a), when the demand grows, the power consumption increases in all three methods. MadVM has less power consumption than the baseline methods, i.e. $\text{MadVM} < \text{CompVM} < \text{CloudScale}$. As CompVM and CloudScale mainly consider the initial deployment with a predicted pattern, they may result in failing to capture the dynamics of the demand when the transition pattern changes. MadVM adopts an online learning based approach to compute the transition probabilities, and the dynamics can always be captured. In Fig. 4(b), while increasing the demand, all methods use more PMs and hence consume more power. MadVM uses the least PMs among the three, which also gives $\text{MadVM} < \text{CompVM} < \text{CloudScale}$. This reflects that the resource utilization in MadVM is the highest. The average power consumption and the number of PMs used in the PlanetLab trace for the three methods are similar to the results with the Google trace, i.e. $\text{MadVM} < \text{CompVM} < \text{CloudScale}$. We omit them here to save space.

Fig. 4(c) and 5(a) show the average resource shortage over time in the two traces. While the resource demand increases, the resource shortage grows in all three methods (MadVM with a large λ , CompVM and CloudScale). They all have a very low average resource shortage ($< 1\%$ in the Google trace and $< 3.5\%$ in the PlanetLab trace) following the pattern $\text{MadVM} \approx \text{CompVM} < \text{CloudScale}$. Because the resource demand in the PlanetLab trace fluctuates more

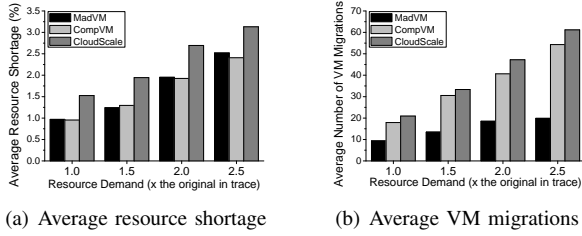


Fig. 5. Performance in the PlanetLab Trace

intensely than that in the Google trace, it is harder to catch the dynamics. Hence all three methods show higher average resource shortage in the PlanetLab trace.

Fig. 4(d) and 5(b) illustrate the average VM migrations per time-slot. As the demand of VMs increases, the number of VM migrations also increases, which follows $\text{CompVM} < \text{MadVM} < \text{CloudScale}$ in Fig. 4(d). As both CompVM and CloudScale trigger VM migrations when resource shortage appears, they migrate more VMs with the increase of resource shortage. Instead of taking VM migration as a remedy, MadVM takes it as a management method to utilize the resources more efficiently. Thus, it is reasonable for MadVM to adopt more VM migrations than CompVM in Fig. 4(d). As demonstrated in Fig. 5(a), the average resource shortage in PlanetLab is relatively high, so the two baseline algorithms trigger many more VM migrations. Thus, in Fig. 5(b), the result follows $\text{MadVM} < \text{CompVM} < \text{CloudScale}$. Therefore, we can say MadVM manages the VMs more efficiently so that it needs fewer VM migrations to keep to the same average resource shortage when the demand fluctuates widely.

In summary, while maintaining the resource shortage nearly to 0, MadVM can reduce the power consumption by up to 23% and 47% (averagely 19% and 42%) compared with CompVM and CloudScale, respectively. Moreover, the more widely the demands fluctuate, the better performance MadVM achieves in the power consumption and the frequency of VM migrations.

E. Resource Shortage under Insufficient Number of PMs

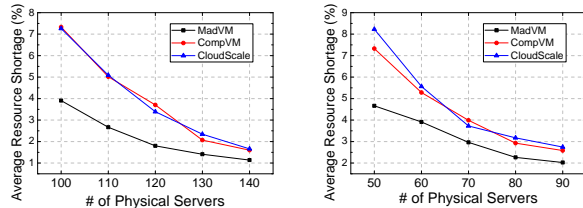


Fig. 6. Average resource shortage under different number of PMs

When setting a large λ in MadVM, all three methods have very low resource shortage. Here, we assume the number of PMs less than the demand of the VMs, so that we can observe the resource shortage among the three methods. Figure 6(a) and 6(b) show the resource shortage under twice of the original resource demands in the traces. As the number of PMs increases, the average resource shortage decreases as expected. CompVM and CloudScale have a similar resource shortage as

they adopt a similar greedy strategy when resource shortage appears. As MadVM can capture the temporal correlation of the resource demand, the resource shortage can be predicted and avoided. Thus, MadVM has a significantly lower shortage, i.e., averagely 34% smaller than the two baseline algorithms. Moreover, since MadVM adopts optimization based approach to manage the VMs, it can find the optimal policy under local observation of each VM. Therefore, we can say MadVM has the most efficient utilization of the resources.

V. CONCLUSION

In this paper, we study dynamic VM management as a large-scale MDP problem. By analyzing the Google workload trace, we show that the resource demands of VMs are quasi-static over time. We first derive an exponential-time optimal algorithm to solve the problem. Then, we adopt approximate MDP and propose an efficient learning-based approximate management approach, called MadVM. MadVM can capture the temporal correlation of a VM's resource demand. Moreover, by allowing a small amount of information sharing, MadVM can be implemented in distributed fashion, which can help improve the robustness and scalability of data centers. The simulations based on two real-world workload traces show significant performance gains by the proposed MadVM over two existing baseline approaches in power consumption, resource shortage and the number of VM migrations. Here, we consider only optimization of VM allocation. In the future, we may consider a joint multi-level optimization including CPU scheduling, the allocation of VMs and the cost of VM migration to achieve energy saving in data centers.

APPENDIX A PROOF OF LEMMA 2

Proof. We define $S_{i,l}$ as the state of the VM m_l in the state $S_i \in \mathbb{S}$. By applying the linear approximation structure in Eqn. (20), the equivalent Bellman's equation in Eqn. (12) can be

written as follows, $\forall S_i \in \mathbb{S}$

$$\begin{aligned}
\beta + V(S_i) &= \min_{\gamma \in \mathcal{A}(\mathbf{S}_i)} \{g(S_i) + \sum_{S_j \in \mathbb{S}} Pr[S_j|S_i, \gamma] V(S_j)\} \\
&\approx \min_{\gamma \in \mathcal{A}(\mathbf{S}_i)} \{g(S_i) + \sum_{S_j \in \mathbb{S}} Pr[S_j|S_i, \gamma] \sum_{l=1}^{|V_m|} \tilde{V}_l(S_{i,l})\} \\
&= g(S_i) + \min_{\gamma \in \mathcal{A}(\mathbf{S}_i)} \left\{ \sum_{l=1}^{|V_m|} \sum_{S_j \in \mathbb{S}} \left(\prod_{n=1}^{|V_m|} Pr[S_{j,n}|S_{i,n}, \gamma_n] \right) \tilde{V}_l(S_{i,l}) \right\} \\
&= g(S_i) + \min_{\gamma \in \mathcal{A}(\mathbf{S}_i)} \left\{ \sum_{l=1}^{|V_m|} \sum_{S_j \in \mathbb{S}} (Pr[S_{j,l}|S_{i,l}, \gamma_l] \cdot \right. \\
&\quad \left. \prod_{n=1, n \neq l}^{|V_m|} Pr[S_{j,n}|S_{i,n}, \gamma_n]) \tilde{V}_l(S_{i,l}) \right\} \\
&= g(S_i) + \min_{\gamma \in \mathcal{A}(\mathbf{S}_i)} \left\{ \sum_{l=1}^{|V_m|} \sum_{S'_j \in \mathcal{S}_K^l} (Pr[S'_j|S_i, \gamma_l] \tilde{V}_l(S'_j)) \right\} \\
&= \sum_{l=1}^{|V_m|} \left(g(S_i) + \min_{\gamma_l \in \mathcal{A}_l(\mathbf{S}_i)} \left\{ \sum_{S'_j \in \mathcal{S}_K^l} Pr[S'_j|S_i, \gamma_l] \tilde{V}_l(S'_j) \right\} \right).
\end{aligned}$$

This completes the proof. \square

APPENDIX B PROOF OF THEOREM 1

Proof. For any admissible policy $\{\gamma_0, \gamma_1, \dots\}$ there exists an $\epsilon > 0$ and a positive integer m such that

$$[\tilde{\mathbf{P}}_{\mu_m} \tilde{\mathbf{P}}_{\mu_{m-1}} \dots \tilde{\mathbf{P}}_{\mu_1}]_{ir} \geq \epsilon \quad i = 1, \dots, |\mathbb{S}|, \text{ and} \quad (34)$$

$$[\tilde{\mathbf{P}}_{\mu_{m-1}} \tilde{\mathbf{P}}_{\mu_{m-2}} \dots \tilde{\mathbf{P}}_{\mu_0}]_{ir} \geq \epsilon \quad i = 1, \dots, |\mathbb{S}| \quad (35)$$

where $[\cdot]_{ir}$ denotes the element of i^{th} row and j^{th} column of corresponding matrix. We denote $\delta^k(\mathbf{S}^i) = \tilde{\mathbf{V}}_l^{k+1}(\mathbf{S}^i) - \tilde{\mathbf{V}}_l^k(\mathbf{S}^i)$. We denote the k^{th} value iteration as follows:

$$\mathcal{F}_{(k)}(\mathbf{S}_i) = \min_{\gamma} \left[g(\mathbf{S}_i) + \sum_j Pr[\mathbf{S}_j|\mathbf{S}_i, \gamma] \tilde{\mathbf{V}}_l^k(\mathbf{S}_j) \right]. \quad (36)$$

Set $\lambda_{(k)} = \mathcal{F}_{(k)}(\mathbf{S}_r)$. Then we have

$$\tilde{\mathbf{V}}_l^{k+1} = \mathbf{g} + \tilde{\mathbf{P}}_{\gamma_k} \tilde{\mathbf{V}}_l^k - \lambda_k \mathbf{e} \leq g + \tilde{\mathbf{P}}_{\gamma_{k-1}} \tilde{\mathbf{V}}_l^k - \lambda_k \mathbf{e}, \quad (37)$$

$$\tilde{\mathbf{V}}_l^k = \mathbf{g} + \tilde{\mathbf{P}}_{\gamma_{k-1}} \tilde{\mathbf{V}}_l^{k-1} - \lambda_{k-1} \mathbf{e} \leq g + \tilde{\mathbf{P}}_{\gamma_k} \tilde{\mathbf{V}}_l^{k-1} - \lambda_{k-1} \mathbf{e}. \quad (38)$$

With the definition $\delta^k(\mathbf{S}^i) = \tilde{\mathbf{V}}_l^{k+1}(\mathbf{S}^i) - \tilde{\mathbf{V}}_l^k(\mathbf{S}^i)$, we obtain

$$\tilde{\mathbf{P}}_{\gamma_k} \delta^{k-1} + (\lambda_{k-1} - \lambda_k) \mathbf{e} \leq \delta^k \leq \tilde{\mathbf{P}}_{\gamma_{k-1}} \delta^{k-1} + (\lambda_{k-1} - \lambda_k) \mathbf{e}. \quad (39)$$

By iterating, we have

$$\begin{aligned}
\tilde{\mathbf{P}}_{\gamma_k} \dots \tilde{\mathbf{P}}_{\gamma_{k-m+1}} \delta^{k-m} + (\lambda_{k-m} - \lambda_k) \mathbf{e} &\leq \delta^k \\
&\leq \tilde{\mathbf{P}}_{\gamma_{k-1}} \dots \tilde{\mathbf{P}}_{\gamma_{k-m}} \delta^{k-m} + (\lambda_{k-m} - \lambda_k) \mathbf{e}.
\end{aligned} \quad (40)$$

Due to (34) and (35), the R.H.S. of (39) yields

$$\delta^k(\mathbf{S}_i) \leq \sum_{\mathbf{S}_j \in \mathbb{S}} [\tilde{\mathbf{P}}_{\gamma_k} \dots \tilde{\mathbf{P}}_{\gamma_{k-m+1}}]_{ij} \delta^{k-m}(\mathbf{S}_j) + \lambda_{k-m} - \lambda_k \quad (41)$$

$$\Rightarrow \delta^k(\mathbf{S}_i) \leq (1 - \epsilon) \max_j \delta^{k-m}(\mathbf{S}_j) + \lambda_{k-m} - \lambda_k. \quad (42)$$

Therefore, we obtain

$$\max_j \delta^k(\mathbf{S}_j) \leq (1 - \epsilon) \max_j \delta^{k-m}(\mathbf{S}_j) + \lambda_{k-m} - \lambda_k. \quad (43)$$

Similarly, from the L.H.S. of (39) we obtain

$$\min_j \delta^k(\mathbf{S}_j) \geq (1 - \epsilon) \min_j \delta^{k-m}(\mathbf{S}_j) + \lambda_{k-m} - \lambda_k. \quad (44)$$

By combining (43) and (44), we have

$$\begin{aligned}
\max_i \delta^k(\mathbf{S}_i) - \min_i \delta^k(\mathbf{S}_i) &\leq \\
(1 - \epsilon) (\max_i \delta^{k-m}(\mathbf{S}_i) - \min_i \delta^{k-m}(\mathbf{S}_i)) &\quad (45)
\end{aligned}$$

For some $B > 0$ and all k , we have

$$\max_i \delta^k(\mathbf{S}_i) - \min_i \delta^k(\mathbf{S}_i) \leq B(1 - \epsilon)^{k/m}. \quad (46)$$

Since $\delta^k(\mathbf{S}_i) = 0$, it follows that

$$\begin{aligned}
|\tilde{\mathbf{V}}_l^k(\mathbf{S}_i) - \tilde{\mathbf{V}}_l^k(\mathbf{S}_i)| &= |\delta^k(\mathbf{S}_i)| \leq \\
\max_j \delta^k(\mathbf{S}_j) - \min_j \delta^k(\mathbf{S}_j) &\leq B(1 - \epsilon)^{k/m}. \quad (47)
\end{aligned}$$

Therefore, for every $n > 1$ and \mathbf{S}_i we have

$$\begin{aligned}
|\tilde{\mathbf{V}}_l^{k+n}(\mathbf{S}_i) - \tilde{\mathbf{V}}_l^k(\mathbf{S}_i)| &\leq \sum_{j=0}^{n-1} |\tilde{\mathbf{V}}_l^{k+j+1}(\mathbf{S}_i) - \tilde{\mathbf{V}}_l^{k+j}(\mathbf{S}_i)| \\
&\leq B(1 - \epsilon)^{k/m} \sum_{j=0}^{n-1} (1 - \epsilon)^{j/m} \\
&= \frac{B(1 - \epsilon)^{k/m} (1 - (1 - \epsilon)^{n/m})}{1 - (1 - \epsilon)^{1/m}}, \quad (48)
\end{aligned}$$

so $\tilde{\mathbf{V}}_l^k(\mathbf{S}_i)$ is a Cauchy sequence and converges to a limit $\tilde{\mathbf{V}}_l^*(\mathbf{S}_i)$. Therefore, we obtain the equation (28). This completes the proof. \square

APPENDIX C PROOF OF THEOREM 2

The lower-bound is straightforward. The proof of the upper-bound is given below. Since

$$\begin{aligned}
\|\mathbf{W}^\infty - \mathbf{X}^*\| &\leq \|\tilde{\mathbf{F}}^n(\mathbf{W}^\infty) - \tilde{\mathbf{F}}^n(\mathbf{X}^*)\| + \|\tilde{\mathbf{F}}^n(\mathbf{X}^*) - \mathbf{X}^*\| \\
&\leq \beta \|\mathbf{W}^\infty - \mathbf{X}^*\| + \|\tilde{\mathbf{F}}^n(\mathbf{X}^*) - \mathbf{X}^*\|,
\end{aligned}$$

we have

$$\|\mathbf{W}^\infty - \mathbf{X}^*\| \leq \frac{1}{1 - \beta} \|\tilde{\mathbf{F}}^n(\mathbf{X}^*) - \mathbf{X}^*\|. \quad (49)$$

From the definition of constant c , we have

$$\begin{aligned}
\|\tilde{\mathbf{F}}^n(\mathbf{X}^*) - \mathbf{X}^*\| &\leq \|\tilde{\mathbf{F}}^n(\mathbf{X}^*) - \mathbf{M}^\dagger \mathbf{V}^*\| + \|\mathbf{M}^\dagger \mathbf{V}^* - \mathbf{X}^*\| \\
&\leq c \|\tilde{\mathbf{F}}^{n-1}(\mathbf{X}^*) - \mathbf{M}^\dagger \mathbf{V}^*\| + \|\mathbf{M}^\dagger \mathbf{V}^* - \mathbf{X}^*\| \\
&\leq (c^n + 1) \|\mathbf{M}^\dagger \mathbf{V}^* - \mathbf{X}^*\|. \quad (50)
\end{aligned}$$

As a result,

$$\begin{aligned}
\|\mathbf{M}\mathbf{W}^\infty - \mathbf{V}^*\| &\leq \|\mathbf{M}\mathbf{W}^\infty - \mathbf{M}\mathbf{X}^*\| + \|\mathbf{M}\mathbf{X}^* - \mathbf{V}^*\| \\
&\leq a\|\mathbf{W}^\infty - \mathbf{X}^*\| + \|\mathbf{M}\mathbf{X}^* - \mathbf{V}^*\| \\
&\leq \frac{a(c^n + 1)}{1 - \beta} \|\mathbf{M}^\dagger \mathbf{V}^* - \mathbf{X}^*\| \\
&\quad + \|\mathbf{M}\mathbf{X}^* - \mathbf{V}^*\|,
\end{aligned}$$

where the last inequality is because of (49) and (50). This completes the proof.

REFERENCES

- [1] X. Li, J. Wu, S. Tang, and S. Lu, "Let's stay together: Towards traffic aware virtual machine placement in data centers," in *INFOCOM 2014*.
- [2] J.-J. Kuo, H.-H. Yang, and M.-J. Tsai, "Optimal approximation algorithm of virtual machine placement for data latency minimization in cloud systems," in *INFOCOM 2014*.
- [3] R. Nathuji and K. Schwan, "Virtualpower: coordinated power management in virtualized enterprise systems," in *SIGOPS 2007*.
- [4] L. Popa, G. Kumar, M. Chowdhury, A. Krishnamurthy, S. Ratnasamy, and I. Stoica, "Faircloud: sharing the network in cloud computing," in *SIGCOMM 2012*.
- [5] M. Alicherry and T. Lakshman, "Optimizing data access latencies in cloud systems by intelligent virtual machine placement," in *INFOCOM 2013*.
- [6] Y. Guo, A. L. Stolyar, and A. Walid, "Shadow-routing based dynamic algorithms for virtual machine placement in a network cloud," in *INFOCOM 2013*.
- [7] R. Cohen, L. Lewin-Eytan, J. Naor, and d. raz, "Almost optimal virtual machine placement for traffic intense data centers," in *INFOCOM 2013*.
- [8] H. Jin, D. Pan, J. Xu, and N. Pissinou, "Efficient VM placement with multiple deterministic and stochastic resources in data centers," in *GLOBECOM 2012*.
- [9] N. Bobroff, A. Kochut, and K. Beaty, "Dynamic placement of virtual machines for managing sla violations," in *IM 2007*.
- [10] Z. Shen, S. Subbiah, X. Gu, and J. Wilkes, "Cloudscale: elastic resource scaling for multi-tenant cloud systems," in *SOCC 2011*.
- [11] A. Beloglazov and R. Buyya, "Energy efficient resource management in virtualized cloud data centers," in *CCGrid 2010*.
- [12] L. Chen and H. Shen, "Consolidating complementary VMs with spatial/temporal-awareness in cloud datacenters," in *INFOCOM 2014*.
- [13] A. Beloglazov and R. Buyya, "Managing overloaded hosts for dynamic consolidation of virtual machines in cloud data centers under quality of service constraints," *IEEE TPDS*, vol. 24, no. 7, pp. 1366–1379, 2013.
- [14] R. Buyya, A. Beloglazov, and J. Abawajy, "Energy-efficient management of data center resources for cloud computing: A vision, architectural elements, and open challenges," in *PDPTA 2010*.
- [15] Q. Zhang, M. F. Zhani, R. Boutaba, and J. L. Hellerstein, "Dynamic heterogeneity-aware resource provisioning in the cloud," *IEEE Transactions on Cloud Computing*, vol. 2, no. 1, Mar. 2014.
- [16] "Xen Project," <http://www.xenproject.org/>.
- [17] "Kernel Based Virtual Machine," <http://www.linux-kvm.org/>.
- [18] D. P. Bertsekas, D. P. Bertsekas, D. P. Bertsekas, and D. P. Bertsekas, *Dynamic programming and optimal control*, 1995, vol. 2, no. 3.
- [19] R. Bellman, *Dynamic Programming*. Princeton University Press, 1957.
- [20] Y. Cui, V. K. Lau, R. Wang, H. Huang, and S. Zhang, "A survey on delay-aware resource control for wireless systems large deviation theory, stochastic Lyapunov drift, and distributed stochastic learning," *IEEE Trans. on Information Theory*, vol. 58, no. 3, pp. 1677–1701, 2012.
- [21] "Google cluster data," <https://code.google.com/p/googleclusterdata/>.
- [22] R. N. Calheiros, R. Ranjan, A. Beloglazov, C. A. De Rose, and R. Buyya, "Cloudsim: a toolkit for modeling and simulation of cloud computing environments and evaluation of resource provisioning algorithms," *Software: Prac. and Exp.*, vol. 41, no. 1, pp. 23–50, 2011.